HAL
open science

A case study of optimal input-output system with sampled-data control: Ding et al. force and fatigue muscular control model

Toufik Bakir, Bernard Bonnard, Jérémy Rouot

To cite this version:

Toufik Bakir, Bernard Bonnard, Jérémy Rouot. A case study of optimal input-output system with sampled-data control: Ding et al. force and fatigue muscular control model. Networks and Heterogeneous Media, 2019, 14 (1), pp.79-100. 10.3934/nhm.2019005 . hal-01779349v2

HAL Id: hal-01779349

https://inria.hal.science/hal-01779349v2

Submitted on 26 Apr 2018

HAL is a multi-disciplinary open access archive for the deposit and dissemination of scientific research documents, whether they are published or not. The documents may come from teaching and research institutions in France or abroad, or from public or private research centers.

L'archive ouverte pluridisciplinaire **HAL**, est destinée au dépôt et à la diffusion de documents scientifiques de niveau recherche, publiés ou non, émanant des établissements d'enseignement et de recherche français ou étrangers, des laboratoires publics ou privés.

Manuscript submitted to
AIMS' Journals
Volume **X**, Number **0X**, XX **200X**

doi:10.3934/xx.xx.xx.xx

pp. **X–XX**

A CASE STUDY OF OPTIMAL INPUT-OUTPUT SYSTEM WITH SAMPLED-DATA CONTROL: DING ET AL. FORCE AND FATIGUE MUSCULAR CONTROL MODEL

Abstract. The objective of this article is to make the analysis of the muscular force response to optimize electrical pulses trains using Ding et al. force-fatigue model. A geometric analysis of the dynamics is provided and very preliminary results are presented in the frame of optimal control using a simplified input-output model. In parallel, to take into account the physical constraints of the problem, partial state observation and input restrictions, an optimized pulses train is computed with a model predictive control, where a nonlinear observer is used to estimate the state-variables.

Toufik Bakir

Le2i Laboratory FRE 2005, CNRS
Dijon, France

Bernard Bonnard

Univ. Bourgogne Franche-Comté and INRIA Sophia Antipolis,
Dijon, France

Jérémy Rouot*

EPF École Ingénieur-e-s
Troyes, France

(Communicated by the associate editor name)

1. **Introduction.** Functional Electrical Stimulation (FES) consists of applying an electrical stimulation to the muscle, in order to produce functional movements. It can be used for the muscular reinforcement, reeducation of the muscle and in the case of paralysis to activate the paralyzed muscles to produce movements. Mathematically FES leads to a sampled-data control problem which can be analyzed in this framework.

The simulations of muscular response to electrical stimulations are based on dynamics models. The origin comes from the Hill-Langmuir equation in the context of biochemistry and pharmacology, see [12]. More recent models in the framework of model identification in non linear control are to due Bobet and Stein [2] and Law and Shields [15] and in this context a more sophisticated model was proposed by Ding et al. [6, 7, 8, 9] where the force model is coupled to a fatigue model. This led to a set of five differential equations with a sampled-data control which can be used to stimulate and to control the force response to a pulses train of electrical

2010 *Mathematics Subject Classification.* 49K15, 93B07, 92B05.

Key words and phrases. Muscular Force and Fatigue model, Optimization of sampled-data control, Non linear observer, Model predictive control.

The first author is supported by NSF grant xx-xxxx.

*∗ Corresponding author: xxxx.

stimulations and we shall refer to this model as the Ding et al. force-fatigue model in the sequel.

Only few works used this model to design an optimized train of pulses to control the force level [6, 7, 8, 9]. Our aim being to make a more complete study of the problem in the framework of non linear optimal control, using sampled-data controls.

A geometric analysis of the model is provided and preliminary results in the frame of optimal control with sampled-data control [3]. It is based on a simplified dynamics using the geometric properties of the force-fatigue model and control reduction to simplify the physical control constraints. The complete system is analyzed in details using a control predictive strategy (MPC), see [17, 19] coupled with a non linear observer technique based on [11] to estimate the state variable. This study completes [1] and gives non trivial optimized pulses trains which can be implemented in practise up to specific devices to speed on line numerical computations.

The article is organized as follows. In Section 2, we make a brief presentation of Ding et al. force-fatigue model based on [20]. In Section 3, the dynamics of the force model is briefly investigated to describe the input-output properties. In Section 4, the force-fatigue model is analyzed in the framework of geometric optimal sampled-data control systems and preliminary results are presented using a simplified model using a model reduction and an input transformation. Section 5 is devoted to the observer description. In Section 6, MPC method is presented using a further discretization of the dynamics to conclude by the algorithm used to compute in practise the optimized pulses trains. Numerical results are presented in the final Section 7.

2. **Mathematical force-fatigue model.** We refer to [20] for a complete description and discussions of the model. The Ding et al. model studied in this article is presented next in the framework of model dynamics construction based on input-output observation and using the so-called *tetania* phenomenon in muscles responses. The first part of the model is the force (output) to pulses electrical stimulations (input). The pulses are normalized Dirac impulses at times $0 = t_1 < t_2 < \ldots < t_n$:

$$v(t) = \sum_{i=1}^{n} \delta(t - t_i)$$

and $I_i = t_i - t_{i-1}$ is the interpulse and convexifying leads to apply the input:

$$v(t) = \sum_{i=1}^{n} \eta_i \, \delta(t - t_i).$$

for some amplitudes $\eta_i \in [0, 1],\ i \in \{1, \ldots, n\}$. Such pulses train feeds a first order model to produce an output according to the dynamics

$$\dot{u}(t) + \frac{u(t)}{\tau_c} = \sum_{i=1}^{n} R_i \eta_i \delta(t - t_i) \tag{1}$$

where R_i is a scaling factor associated to the phenomenon of tetania and corresponds to a accumulated effect of successive pulses and is modeled as

$$R_i = \begin{cases} 1 & \text{for } i = 1 \\ 1 + (R_0 - 1)\, \exp\left(-\frac{t_{i+1} - t_i}{\tau_c}\right) & \text{for } i > 1 \end{cases}$$

where the magnitude is characterized by R_0 which is the limit case to high-frequency pulse. We denote $E_s(t) = u(t)$ the response to the pulses train and which is the (physical) control variable. It is of the form

$$E_s(t) = \frac{1}{\tau_c} \sum_{i=1}^{n} R_i \eta_i H(t - t_i) \exp\left(-\frac{t - t_i}{\tau_c}\right) \tag{2}$$

where $H(t - t_i) = \begin{cases} 0 \text{ if } t < t_i \\ 1 \text{ if } t \geq t_i \end{cases}$ is the Heaviside function.

The force response to such a train is modelled by the two equations of the so-called *force model*:

$$\frac{\mathrm{d}C_N}{\mathrm{d}t} + \frac{C_N}{\tau_c} = E_s(t) \tag{3}$$

which corresponds to a first order (resonant) linear dynamics which can be integrated with $C_N(0) = 0$ and the force response $F(t)$ is described by the equation

$$\frac{\mathrm{d}F}{\mathrm{d}t} = A\,a - F\,b \tag{4}$$

where A is a fatigue parameter. Non-linear features of the model are described by the two mappings a, b:

$$a = \frac{C_N}{K_m + C_N}, \quad b = \frac{1}{\tau_1 + \tau_2\,a} \tag{5}$$

where K_m, τ_1 are fatigue parameters and τ_2 an additional constant.

The complete model is obtained by describing the evolutions of the parameters associated to *fatigue* and corresponds to the *linear dynamics*

$$\frac{\mathrm{d}A}{\mathrm{d}t} = -\frac{A - A_{rest}}{\tau_{fat}} + \alpha_A\,F \tag{6}$$

$$\frac{\mathrm{d}K_m}{\mathrm{d}t} = -\frac{K_m - K_{m,rest}}{\tau_{fat}} + \alpha_{K_m}\,F \tag{7}$$

$$\frac{\mathrm{d}\tau_1}{\mathrm{d}t} = -\frac{\tau_1 - \tau_{1,rest}}{\tau_{fat}} + \alpha_{\tau_1}\,F. \tag{8}$$

The full set of equations (3)-(4)-(6)-(7)-(8) are the *force and fatigue model*.

We refer to Table 1 for the definitions and details of the symbols of the force-fatigue model.

For the purpose of our analysis the force fatigue model is written as the single-input control system:

$$\frac{\mathrm{d}x}{\mathrm{d}t} = F_0(x) + u\,F_1(x) \tag{9}$$

with $x = (x_1, x_2, x_3, x_4, x_5) = (C_N, F, A, K_m, \tau_1)$ where u denotes the control $u = E_s(t)$ corresponding to the *sampled physical control data*:

$$(I_1, I_2, \ldots, I_n, \eta_1, \ldots, \eta_n) \tag{10}$$

with constraints

$$I_{\min} \leq I_i \leq I_{\max}, \quad 0 \leq \eta_i \leq 1$$

corresponding to interpulses bounds and amplitude convexification. This leads to a *non linear model* with sampled control data with prescribed *convex control constraints* $(\eta, I) \in C;\ \eta = (\eta_1, \ldots, \eta_n),\ I = (I_1, \ldots, I_n)$.

3. **The force model.** The force model can be briefly investigated to describe preliminary results.

TABLE 1. Margin settings

Symbol	Unit	Value	description
C_N	—	—	Normalized amount of Ca^{2+}-troponin complex
F	N	—	Force generated by muscle
t_i	ms	—	Time of the ith pulse
n	—	—	Total number of the pulses before time t
i	—	—	Stimulation pulse index
τ_c	ms	20	Time constant that commands the rise and the decay of C_N
R_0	—	1.143	Term of the enhancement in C_N from successive stimuli
A	$\frac{N}{ms}$	—	Scaling factor for the force and the shortening velocity of muscle
τ_1	ms	—	Force decline time constant when strongly bound cross-bridges absent
τ_2	ms	124.4	Force decline time constant due to friction between actin and myosin
K_m	—	—	Sensitivity of strongly bound cross-bridges to C_N
A_{rest}	$\frac{N}{ms}$	3.009	Value of the parameter A when muscle is not fatigued
$K_{m,rest}$	—	0.103	Value of the parameter K_m when muscle is not fatigued
$\tau_{1,rest}$	ms	50.95	The value of the parameter τ_1 when muscle is not fatigued
α_A	$\frac{1}{ms^2}$	$-4.0\ 10^{-7}$	Coefficient for the force-model parameter A in the fatigue model
α_{K_m}	$\frac{1}{msN}$	$1.9\ 10^{-8}$	Coefficient for the force-model parameter K_m in the fatigue model
α_{τ_1}	$\frac{1}{N}$	$2.1\ 10^{-5}$	Coefficient for force-model parameter τ_1 in the fatigue model
τ_{fat}	s	127	Time constant controlling the recovery of $(A,\ K_m,\ \tau_1)$

3.1. **Parameterization.** Observe that in the force model the static non-linearities described by the mappings a and b can be absorbed by time reparameterization to provide an explicit form for the force responses.

Proposition 1. *The force model can be integrated by quadratures using a time reparameterization.*

Proof. Integrating (3), the equation (4) can be written as

$$\frac{\mathrm{d}F}{\mathrm{d}s} = c(s) - F(s) \tag{11}$$

with $\mathrm{d}s = b(t)\,\mathrm{d}t,\ c = A\,a/b$. □

Thus this gives an explicit force response in the time parameter s

$$(I, \eta, s) \to F(I, \eta, s). \tag{12}$$

Clearly we have

Lemma 3.1. *The above mapping is smooth with respect to I, η and piecewise smooth with respect to s.*

3.2. **Smoothing process.** For the sake of providing a *smooth response* for the observer it is sufficient to smooth the physical sampled control date as follows: use a bump function to smooth each Heaviside mapping $H(t - t_i)$ at the sampling time t_i.

3.3. **Input-simplification.** For the sake of the geometric analysis of the dynamics and to simplify the control constraints on (I, η) the FES signal $E_s(t)$ is taken as the input $u(\cdot)$ of the control system. Using (2) one can write

$$u(t) = E_s(t) = e^{-t/\tau_c}\, v(t)$$

with

$$v(t) = \frac{1}{\tau_c} \sum_{i=1}^{n} H(t - t_i) R_i \eta_i\, e^{t_i/\tau_c}\ . \tag{13}$$

Whence $0 = t_1 < t_2 < \ldots < t_n$ are given $v(t)$ is a piecewise constant control depending upon the parameters $\eta_1, \ldots, \eta_n$ and the dynamics of the force model can be analyzed in the frame of geometric control. Fixing the interpulse led to a sample-data control model.

4. **Force-fatigue control model.** First of all the control system (9) is analyzed in the framework of geometric control.

4.1. **The concepts of geometric control system.** Consider a (smooth) control single-input control system.

$$\begin{cases} \frac{\mathrm{d}x}{\mathrm{d}t} = X(x) + u\,Y(x) \\ y = h(x) \end{cases} \tag{14}$$

where $x \in \mathbb{R}^n$, $y = h(x) \in \mathbb{R}$ corresponds to a (smooth) single-observation mapping. The following concepts rely on seminal results of geometric control, see [18, 13].

We denote $[U, V]$ the Lie bracket of two (smooth) vector fields of $\mathbb{R}^n$:

$$[U, V](x) = \frac{\partial U}{\partial x}\, V(x) - \frac{\partial V}{\partial x}\, U(x)$$

and a vector field U acts on (smooth) mappings f with the Lie derivative:

$$\mathcal{L}_U f = \frac{\partial f}{\partial x}\, U(x).$$

Let $D^1 = \mathrm{span}\{X, Y\}$ and define recursively : $D^k = \mathrm{span}\{D^k \cup [D, D^{k-1}]\},\ k > 1$. Hence D^k represents the Lie brackets of X, Y with lengths smaller than $k + 1$ and

denotes $D_{L.A.} = \text{span} \cup_{k\geq 0} D^k$ is the *Lie algebra generated* by $\{X, Y\}$. The system is called *weakly controllable* if for each $x \in \mathbb{R}^n$, $D_{L.A.}(x) = \mathbb{R}^n$.

The *observation space* is the set of mappings: $\Theta = \{\mathcal{L}_G\, h;\ G \in D_{L.A.}\}$ and the system is called *observable* if for each $x_1, x_2 \in \mathbb{R}^n$, $x_1 \neq x_2$ there exists $g \in \Theta$ such that $g(x_1) \neq g(x_2)$.

Taking $x_0 \in \mathbb{R}^n$, a *frame* at x_0 is a set of elements $X_1, \ldots, X_n$ of $D_{L.A.}$ such that: $X_1, \ldots, X_n$ are linearly independent at x_0 and $\sum_{i=1}^n \text{length}(X_i)$ is minimal.

The system is called *feedback linearizable* in U if $\dot{x} = X(x) + u\,Y(x)$ is feedback equivalent to the linear system $\dot{x} = Ax + ub$, that is there exists a diffeomorphism φ on U, $\varphi(0) = 0$ and a feedback $u = \alpha(x) + \beta(x)\,v$, $\beta(x) \neq 0$ such that $g \cdot (X, Y) = (A, b)$ with $g = (\varphi, \alpha, \beta)$ acting by change of coordinates and (affine) feedback.

Fix $x(0) = x_0$ and $T > 0$ and consider the *extremity mapping*: $E^{x_0,T} : u \in L^\infty([0, T]) \mapsto x(T, x_0, u)$ where $x(\cdot)$ is the response of $\dot{x} = X(x) + u\,Y(x)$ to u defined on $[0, T]$.

The control $u(\cdot)$ is called *singular* on $[0, T]$ if the extremity mapping $E^{x_0,T}$ is not of maximal rank n when evaluated at $u(\cdot)$.

Geometric analysis of an observation system of the form (14) amounts to compute $D_{L.A.}$, the observation space, the singular controls and the feedback equivalence properties. Achievements of geometric optimal controls amounts to synthesize the optimal control in relation with the Lie brackets properties of a frame.

4.2. **Optimal control a force-fatigue model with sampled control data.**

4.2.1. *Concepts.* By the physical nature of the problem, the control in the force/fatigue model (1) is fixed at specific times and remains constant during some period of time. This falls into the framework of sampled-optimal control problem that we recall briefly and we refer to [3] for more details.

Consider a system $\dot{x} = f(x, u)$. When the state $x(\cdot)$ and the control $u(\cdot)$ evolves continuously in time, we speak of a continuous-time optimal control problem and the control is said *permanent*.
When the state $x(\cdot)$ evolves continuously in time whereas the control $u(\cdot)$ evolves in a discrete way, we speak of an *optimal sampled-data control problem*. Denoting by t_f the final time, on $[0, t_f]$ the control u takes its values in a discrete set. That means, for $T > 0$ fixed and $k \in \mathbb{N}$, once the value of $u(kT)$ is chosen, then $u(t) = u(kT)$ for $t \in [kT, (k+1)T]$. T is called the sampling period and $[kT, (k+1)T]$ is the sampling time interval where the control "is freezing".

4.2.2. *Application to the force-fatigue model.* We present the geometric methods presented in [3] and numerical results on a reduced model in dimension 3 related to the force-fatigue model to validate the method.

Consider the minimization problem

$$\int_0^{t_f} \left(u(s)^2 + (F - F_{ref})^2\right) \mathrm{d}s \ \to \min_{|u|\leq 1}$$

subject to the dynamic in $\tilde{x} = (C_N, F, A)$ defined by the equations

$$\begin{aligned} \frac{\mathrm{d}C_N}{\mathrm{d}t} &= -\frac{C_N}{\tau_c} + u \\ \frac{\mathrm{d}F}{\mathrm{d}t} &= a\,A - b\,F \\ \frac{\mathrm{d}A}{\mathrm{d}t} &= -\frac{A - A_{rest}}{\tau_{fat}} + \alpha_A\,F \end{aligned} \tag{15}$$

and to the initial conditions

$$F(0) = A(0) = C_N(0) = 0.$$

The variables $t_f, K_m, \tau_1, \tau_2, \tau_{fat}, \alpha_A, A_{rest}$ are constant and fixed to some ad-hoc values.
The system (15) can be written into the form

$$\dot{\tilde{x}} = \tilde{F}_0(\tilde{x}) + u\,\tilde{F}_1(\tilde{x}).$$

Remark 1. The model (15) is a simplification of the force-fatigue model. In particular, without loss of generality, we don't take into account the factor $\frac{\exp(-t/\tau_c)}{\tau_c}$ appearing in (2). Control constraints $|u| \leq 1$ are not the physical constraints, see Section 3.3. Also the fatigue dynamics is reduced to a single equation, motivated by the controllability properties of the system (6)-(7)-(8).

The permanent control case. The problem considered can be summarized as a permanent optimal control problem as follows

$$\begin{cases} \min \displaystyle\int_0^{t_f} \left(u(s)^2 + (F - F_{ref})^2\right)\,\mathrm{d}s \\ \dot{\tilde{x}} = \tilde{F}_0(\tilde{x}) + u\,\tilde{F}_1(\tilde{x}) \\ u(t) \in [-1, 1] \\ (C_N(0), F(0), A(0)) = (0, 0, 0). \end{cases} \tag{16}$$

The pseudo-Hamiltonian of the system is

$$H(\tilde{x}, p, p^0, u) = p \cdot (\tilde{F}_0(\tilde{x}) + u\,\tilde{F}_1(\tilde{x})) + p^0\,(u^2 + (F - F_{ref})^2)$$

where $(p, p^0) : [0, t_f] \mapsto \mathbb{R}^4$ is the adjoint vector.

We denote by $H_i,\ i = 0, 1$ the Hamiltonian lifts of the vector fields $\tilde{F}_i,\ i = 0, 1$.
Normal case: $p^0 = -1/2$. Applying the Pontryagin maximum principle (PMP), the optimal (permanent) control is given in the normal case by

$$u(t) = \begin{cases} 1 & \text{if } H_1(\tilde{x}(t), p(t)) \geq 1, \\ -1 & \text{if } H_1(\tilde{x}(t), p(t)) < 1, \\ H_1(\tilde{x}(t), p(t)) & \text{otherwise.} \end{cases} \tag{17}$$

Abnormal case: $p^0 = 0$. Abnormal controls are characterized by the equation $H_1 = 0$, which differentiated twice by t leads to

$$p \cdot [\tilde{F}_0, \tilde{F}_1] = 0, \quad p \cdot \Big([[\tilde{F}_0, \tilde{F}_1], \tilde{F}_0] + u\,[[\tilde{F}_0, \tilde{F}_1], \tilde{F}_1]\Big) = 0.$$

Also, we have

$$\begin{aligned} D &= \det(\tilde{F}_1, [\tilde{F}_1, \tilde{F}_0], [[\tilde{F}_1, \tilde{F}_0], \tilde{F}_0]) = -\alpha_A\,(a'(C_N)\,A - b'(C_N)\,F)^2 \\ D' &= \det(\tilde{F}_1, [\tilde{F}_1, \tilde{F}_0], [[\tilde{F}_1, \tilde{F}_0], \tilde{F}_1]) = 0 \end{aligned}$$

and

$$D = 0 \;\Leftrightarrow\; A(C_N(\tau_1+\tau_2)+K_m\tau_1)^2 + F\tau_2(C_N+K_m)^2 = 0.$$

Differentiating one more time led to:

Lemma 4.1. *There are no admissible singular trajectories for the problem* (15).

The sampled-data control case. The corresponding optimal sampled-data control problem is given by

$$\begin{cases} \min \displaystyle\int_0^{t_f} \left(u(kT)^2 + (F-F_{ref})^2\right)\,\mathrm{d}t, \quad \textit{with } k = E(t/T) \\ \dot{\tilde{x}} = \tilde{F}_0(\tilde{x}) + u\,\tilde{F}_1(\tilde{x}) \\ u(k\,T) \in [-1,1] \\ (C_N(0), F(0), A(0)) = (0,0,0). \end{cases} \tag{18}$$

where $T > 0$ is a fixed sampling period such that $t_f = j\,T$ for some $j \in \mathbb{N}$.
Normal case: $p^0 = -1/2$. Following [3], the optimal (sampled-data) control is

$$u(kT) \in \underset{y\in[-1,1]}{arg\,max}\; \frac{1}{T}\int_{kT}^{(k+1)T} H(s,\tilde{x}(s),p(s),p^0,y)\,\mathrm{d}s \tag{19}$$

for all controlling times $kT,\ k \in \{0,\dots,d\}$.

Write

$$\bar{H}_1 = \frac{1}{T}\int_{kT}^{(k+1)T} p_1(s)\,\mathrm{d}s$$

then, the optimal sampled-data control is

$$u(kT) = \begin{cases} 1 & \text{if } \bar{H}_1 > 1, \\ -1 & \text{if } \bar{H}_1 < -1, \\ \bar{H}_1 & \text{otherwise.} \end{cases} \tag{20}$$

Numerical results. In Fig.1, we represent numerical results for several values of t_f/T. The optimal permanent control is represented with thin continuous line. A Gaussian quadrature rule is used to compute $\bar{H}_1$ using approximations of terms of the form $p_1(kT+T), p_1(kT+1/2)\dots$. We observe the convergence of the optimal sampled-data control to the permanent control as T tends to 0.

5. **Observer.** The model used for this study (five state variables) is based on force measurements collected from a set of subjects. Thus, the accuracy of the calculated parameters is directly related to these persons. In this study, we suppose that initial conditions are different following the subject under study. That is why, we need to estimate some of these five initial conditions. Indeed, from a first analysis we can deduce that the rest values $C_N(t_1) = 0$ is well known and don't need estimation. The remaining parameters are A_{rest}, $K_{m,rest}$ and $\tau_{1,rest}$. Concerning $K_{m,rest}$, a sensibility study is realized in order to determine its effect on the force variation.

5.1. **Sensibility study of the force versus K_m:** The force evolution is compared for $K_{m,rest}$ and different values $K'_{m,rest}$ ($\pm 30\%$ of error) for $I = 10ms$, $50ms$ and $100ms$ (see Fig. 2 for $I = 10ms$). In the case of $I = 10ms$, the maximum force error is of -0.3%. Following Interpulse value, the maximum force error is obtained for $I = 100ms$ (-1.3%) which means that a tolerance of $\pm 30\%$ gives force evolution with good accuracy.

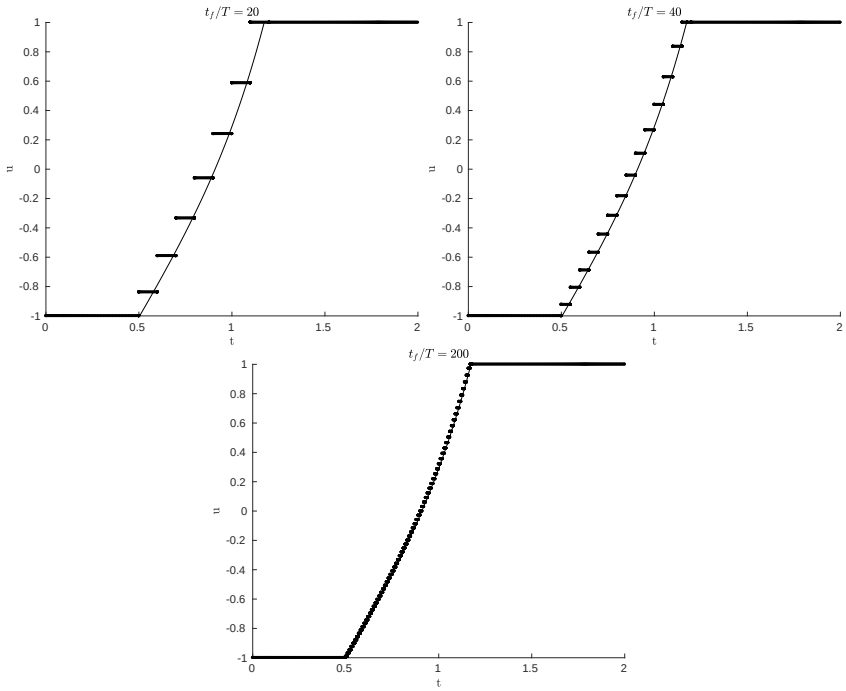

FIGURE 1. Time evolution of the permanent control (thin continuous line) and sampled-data control for several values of the sampling period $T \in \{t_f/20, t_f/40, t_f/200\}$.

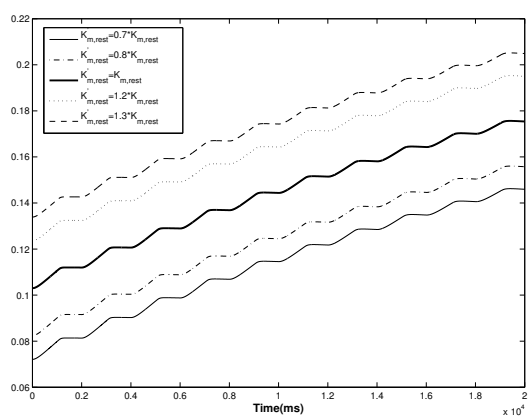

FIGURE 2. Evolution of K_m for different initial conditions (case of $I = 10ms$).

5.2. **High-gain observer synthesis for the estimation of A and τ_1.** In this section, we design a modified version of the standard high-gain observer given in [11] taking into account the specific structure of the problem.
The system defined by the force equation (4) and the fatigue model (6) and (8) can

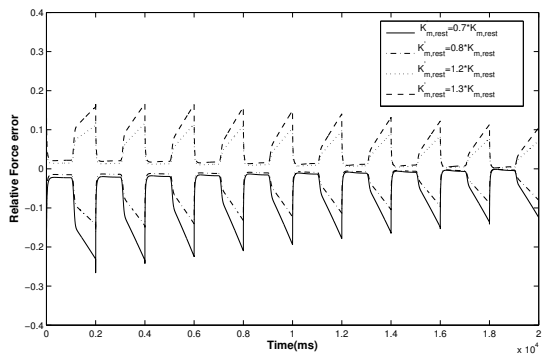

FIGURE 3. Relative error of the force for a well known and erroneous K_m initial condition (case of $I = 10ms$).

be rewritten as the single input-output system:

$$\begin{cases} \dot{x}(t) = \beta^m(t, E_s(t)) f(x(t), E_s(t)) \\ y(t) = h(x(t)) = F(t), \end{cases} \tag{21}$$

with $x = (F, A, \tau_1) \in \mathbb{R}^3$, $y \in \mathbb{R}$, $E_s \in \mathbb{R}$, $\beta = C_N/(C_N + K_m)$, $0 < \beta < 1$, and m is a positive integer. Note that in (21), K_m is not a state variable thanks to the weak sensibility of the solution with respect to this variable (see sensibility study of the force versus K_m). We introduce the change of variables ϕ:

$$\begin{cases} \phi : \mathbb{R}^3 \to \mathbb{R}^3 \\ x \to \phi(x) = [h(x), L_f(h(x)), L_f^2(h(x))]. \end{cases} \tag{22}$$

We have:

$$\frac{\partial \phi}{\partial x} = \begin{pmatrix} 1 & 0 & 0 \\ -\frac{1}{\tau_1+\tau_2\beta} & \beta & \frac{F}{(\tau_1+\tau_2\beta)^2} \\ \frac{\partial L_f^2 h(x)}{\partial x_1} & \frac{\partial L_f^2 h(x)}{\partial x_2} & \frac{\partial L_f^2 h(x)}{\partial x_3} \end{pmatrix}.$$

where

$$\frac{\partial L_f^2 h(x)}{\partial x_1} = \beta\alpha_A + \frac{1}{(x_3+\tau_2\beta)^2}(1 - \frac{x_3-\tau_{1,rest}}{\tau_{fat}} + 2\alpha_{\tau_1} x_1)$$

$$\frac{\partial L_f^2 h(x)}{\partial x_2} = -\beta\frac{\tau_{fat}+x_3+\tau_2\beta}{\tau_{fat}(x_3+\tau_2\beta)}$$

$$\frac{\partial L_f^2 h(x)}{\partial x_3} = \frac{1}{(x_3+\tau_2\beta)^2}(x_2\beta - \frac{x_1}{\tau_{fat}}) - \frac{2x_1}{(x_3+\tau_2\beta)^3}(1 - \frac{x_3-\tau_{1,rest}}{\tau_{fat}} + \alpha_{\tau_1} x_1)$$

and

$$\det(\frac{\partial \phi}{\partial x}) = \frac{\beta(x_2\beta\tau_{fat}(x_3+\tau_2\beta) - \tau_{fat}x_1 + 2x_1(x_3 - \tau_{1,rest} - \alpha_{\tau_1}\tau_{fat}x_1)}{\tau_{fat}(x_3+\tau_2\beta)^3} \tag{23}$$

A sensibility study in (6) and (8) concerning respectively $-\frac{A-A_{rest}}{\tau_{fat}}$ and $-\frac{\tau_1-\tau_{1,rest}}{\tau_{fat}}$, shows that neglecting these two terms induces a maximum error of 7% for A and τ_1, and 6% for the force value. Using the simplified model:

$$\frac{dA}{dt} = \alpha_A F \tag{24}$$

$$\frac{d\tau_1}{dt} = \alpha_{\tau_1} F. \tag{25}$$

with (4) gives:

$$det(\frac{\partial \phi}{\partial x}) = \frac{\beta(x_2\beta(x_3+\tau_2\beta) - x_1 - 2\alpha_{\tau_1}x_1^2)}{(x_3+\tau_2\beta)^3}. \tag{26}$$

Considering the input $E_S(t) \geq 0$, we have

$$\forall t \in [0,T] : (C_N, x_1) \geq 0, (x_2, x_3, K_m) > 0 \Rightarrow (x_3+\tau_2\beta)^3 > 0 \text{ (see 26)}.$$

$$\det(\frac{\partial \phi}{\partial x}) = 0 \Rightarrow \begin{cases} \beta = 0 \Rightarrow C_N = 0 \ (C_N = 0 \Rightarrow x_1 = 0) \ (rest\ time) \\ x_2\beta(x_3+\tau_2\beta) - x_1 - 2\alpha_{\tau_1}x_1^2 = 0 \Rightarrow x_1 = \frac{1 \mp \sqrt{1+8\alpha_{\tau_1}x_2\beta(x_3+\tau_2\beta)}}{4\alpha_{\tau_1}} \end{cases} \tag{27}$$

$\alpha_{\tau_1} \sim 10^{-5}$, $0 \leq \beta \leq 1$ and $(x_3+\tau_2\beta) \sim 10^2$. In the second case of (27), we have

$$8\alpha_{\tau_1}x_2\beta(x_3+\tau_2\beta) << 1 \Rightarrow \left(x_1 = 0 \ (C_N = 0), x_1 = \frac{1}{2\alpha_{\tau_1}}\right).$$

Thus $(\frac{\partial \phi}{\partial x}(\hat{x}(t)) = 0$ for:

- $(C_N, x_1) = 0$ which correponds to the rest time (no control and then no need of state variable estimation).
- $x_1 = \frac{1}{2\alpha_{\tau_1}}$, $x_1 \sim 10^5$ which is outside of force maximum value.

In the simplified model (4),(24) and (25), there is no singularity of $\frac{\partial \phi}{\partial x}(\hat{x}(t))^{-1}$ during stimulation period $(C_N, x_1 > 0)$, and ill-conditioning of the matrix is reduced.

Based on the simplified model, the modified high-gain observer is defined as:

$$\dot{\hat{x}}(t) = \beta^m f_1(\hat{x}(t), E_s(t)) - \beta^m(\frac{\partial \phi}{\partial x}(\hat{x}(t))^{-1}S_\theta^{-1}C^T(C\hat{x}(t) - y(t)). \tag{28}$$

Recall that m is a positive integer. It depends on the used pulses frequency for the stimulation of the muscle. S_θ is a symmetric positive definite matrix given by the following Lyapunov equation:

$$\theta S_\theta(t) + A^T S_\theta(t) + S_\theta(t)A = C^T C \tag{29}$$

where θ is a tuning parameter,

$$A = \begin{pmatrix} 0 & 1 & 0 \\ 0 & 0 & 1 \\ 0 & 0 & 0 \end{pmatrix}, C = \begin{pmatrix} 1 & 0 & 0 \end{pmatrix}.$$

The terms of this matrix $S_\theta = [S_\theta(l,k)]_{1 \leq l,k \leq 3}$ have the following form:

$$S_\theta(l,k) = (-1)^{l+k}\begin{pmatrix} l+k-2 \\ k-1 \end{pmatrix}\theta^{-(l+k-1)}, \quad \begin{pmatrix} n \\ k \end{pmatrix} = \frac{n!}{(n-k)!\,k!}.$$

5.3. **High-gain observer proof.**

$$\begin{cases} \dot{x}(t) = \beta^m(t)f_1(x(t), E_s(t)) \\ \qquad\quad = f(x(t), E_s(t)) \\ y(t) = h(x(t)) \end{cases} \tag{30}$$

$$\begin{aligned} &z_1 = h(x), \quad \dot{z}_1 = L_f h(x) = \beta^m L_{f_1}h(x) = \beta^m z_2, \\ &\dot{z}_2 = L_f(L_{f_1}h(x)) = \beta^m L_{f_1}(L_{f_1}h(x)) = \beta^m z_3, \\ &\vdots \\ &\dot{z}_{n-1} = \beta^m z_n \dot{z}_n = \beta^m L_{f_1}^n h(x) = \varphi_n(u,z) \end{aligned}$$

$$\Rightarrow \begin{pmatrix} \dot{z}_1 \\ \dot{z}_2 \\ \vdots \\ \dot{z}_n \end{pmatrix} = \beta^m \begin{pmatrix} 0 & 1 & \cdots & 0 \\ 0 & \ddots & \ddots & \vdots \\ \vdots & \ddots & \ddots & 1 \\ 0 & \cdots & \cdots & 0 \end{pmatrix} \begin{pmatrix} z_1 \\ z_2 \\ \vdots \\ z_n \end{pmatrix} + \begin{pmatrix} 0 \\ \vdots \\ 0 \\ \varphi_n(u,z) \end{pmatrix} \tag{31}$$

$$\Rightarrow \begin{cases} \dot{z} = \beta^m A z + \varphi(u,z) \\ y = Cz. \end{cases} \tag{32}$$

Take $C = \begin{pmatrix} 1 & 0 & \cdots & 0 \end{pmatrix}$ and consider the system (32). We make the following assumptions

5.4. **Assumptions.**

- H1) $\varphi_n(u,z)$ is globally Lipschitz with respect to z and uniformly with respect to u.
- H2) $\exists\ U \in R$ of admissible controls, a compact $K \in R^n$ and two positive constants β_{min} and β_{max} such that:
  for all $u \in U$ and all $y(t)$ associated to u and initial conditions $z(0) \in K$, we have $\beta_{min} \leq \beta(t) \leq \beta_{max}$.
- H3) $\beta(t)$ is C^1
- H4) $\frac{m\dot{\beta}(t)}{\beta(t)} < 1$

The observer has the following expression:

$$\dot{\hat{z}}(t) = \beta(t)^m A\hat{z}(t) - \beta(t)^m S_\theta^{-1} C^T (C\hat{z}(t) - y(t)) \tag{33}$$

where S_θ is the solution of the Lyapunov equation:

$$\theta S_\theta + A^T S_\theta + S_\theta A - C^T C = 0. \tag{34}$$

The solution of (34) can be rewritten as

$$S_\theta = \frac{1}{\theta} \Delta_\theta\, S_1\, \Delta_\theta. \tag{35}$$

and

$$\Delta_\theta = \mathrm{diag}(1, \frac{1}{\theta} \cdots \frac{1}{\theta^n}) \tag{36}$$

with S_1 is the solution of (34) for $\theta = 1$. Let $\rho = \beta^m$ and $e = \hat{z} - z \Rightarrow \dot{e} = \dot{\hat{z}} - \dot{z}$, then

$$\begin{aligned} \dot{e} &= \rho A\hat{z} + \hat{\varphi}(u,\hat{z}) - S_\theta^{-1} C^T (C\hat{z}(t) - y(t)) - \rho A z - \varphi(u,z) \\ &= \rho(A - S_\theta^{-1} C^T C)e + \hat{\varphi} - \varphi \end{aligned} \tag{37}$$

Write $\bar{e} = \rho \Delta_\theta e$, then

$$\begin{aligned} \dot{\bar{e}} &= \dot{\rho}\Delta_\theta e + \rho \Delta_\theta \dot{e} \\ &= \dot{\rho}\Delta_\theta e + \rho\Delta_\theta(\rho(A - S_\theta^{-1}C^T C)e + \hat{\varphi} - \varphi) \\ &= \dot{\rho}\Delta_\theta e + \rho\Delta_\theta(\rho(A - \theta\Delta_\theta^{-1} S_1^{-1} \Delta_\theta^{-1} \Delta_\theta C^T C \Delta_\theta)e + \hat{\varphi} - \varphi), \quad \Delta_\theta C^T C \Delta_\theta = C^T C \\ &= \frac{\dot{\rho}}{\rho}\bar{e} + \rho\theta A\bar{e} - \theta S_1^{-1} C^T C\bar{e} + \rho\Delta_\theta(\hat{\varphi} - \varphi), \quad \Delta_\theta A \Delta_\theta^{-1} = \theta A \end{aligned} \tag{38}$$

Consider the Lyapunov function: $V = \bar{e}^T S_1 \bar{e}$. Then

$$\begin{aligned} \dot{V} &= 2\bar{e}^T S_1 \dot{\bar{e}} \\ &= 2\bar{e}^T S_1 (\frac{\dot{\rho}}{\rho}\bar{e} + \rho\theta A\bar{e} - \theta S_1^{-1} C^T C\bar{e} + \rho\Delta_\theta(\hat{\varphi} - \varphi)) \end{aligned} \tag{39}$$

$2\bar{e}^T S_1 A\bar{e} = \bar{e}^T (S_1 A + A^T S_1)\bar{e}$ and $S_1 A + A^T S_1 = -S_1 + C^T C$.
Then, we have

$$\begin{aligned} \dot{V} &= -\theta\rho V + \theta\rho\bar{e}^T C^T C\bar{e} - 2\bar{e}^T C^T C\bar{e} + 2\bar{e}^T S_1 \frac{\dot{\rho}}{\rho}\bar{e} + 2\bar{e}^T S_1 \rho\Delta_\theta(\hat{\varphi} - \varphi) \\ &= -\theta\rho V + (\theta\rho - 2) \mid\mid C\bar{e} \mid\mid^2 + 2\frac{\dot{\rho}}{\rho} V + 2\bar{e}^T S_1 \rho\Delta_\theta(\hat{\varphi} - \varphi) \\ &= -(\theta\rho - 2\frac{\dot{\rho}}{\rho})V + (\theta\rho - 2) \mid\mid C\bar{e} \mid\mid^2 + 2\bar{e}^T S_1 \rho\Delta_\theta(\hat{\varphi} - \varphi) \end{aligned} \tag{40}$$

We deduce that

$$\begin{aligned} &\theta\rho - 2\frac{\dot{\rho}}{\rho} > 0 \Rightarrow \theta > 2\frac{\dot{\rho}}{\rho^2}, \\ &\theta\rho - 2 < 0 \Rightarrow \theta < \frac{2}{\rho} \Rightarrow 2\frac{\dot{\rho}}{\rho^2} < \theta < \frac{2}{\rho} \\ &\Rightarrow (\frac{\dot{\rho}}{\rho} = m\frac{\dot{\beta}}{\beta}) < 1. \end{aligned} \tag{41}$$

Using (41) and assymption H1:

$$\begin{aligned} \dot{V} &\leq -\gamma V + 2\bar{e}^T S_1 \rho\Delta_\theta \mid\mid \hat{\varphi} - \varphi \mid\mid, \quad \gamma > 0 \\ &\leq -\gamma V + 2\bar{e}^T S_1 \frac{\rho}{\theta^n} \mid \hat{\varphi_n} - \varphi_n \mid \\ &\leq -\gamma V + 2\bar{e}^T S_1 \frac{\rho}{\theta^n} K\bar{e} \\ &\leq -(\gamma - \frac{\beta^m}{\theta^n} K_1)V. \end{aligned} \tag{42}$$

For m and θ sufficiently large: $\gamma > \frac{\beta^m}{\theta^n} K_1 \Rightarrow \dot{V} \leq -\gamma_1 V, \quad \gamma_1 > 0$.

In the particular case of the force fatigue model, $\beta(t)$ is piecewise smooth, the lack of regularity is numerically bypassed by the choice of the integer m. For example, for $I = 10ms$, $m = 3$ is sufficient to estimate the whole variables. However, for $I = 25ms$, m must be at least equal to 5 (see observer simulations in Section 7).

6. **Model predictive control (MPC).** MPC computes a sequence of future controls to optimize "future" plant behavior (see Fig. 4). This computation is based on the dynamic model of the system, and must respect a certain cost and associated constraints (optimal control).
In this framework, Model Predictive Heuristic Control (MPHC) was introduced by Richalet et al. [17] using impulse response type dynamic model. Dynamic Matrix Control (DMC) followed in 1980 (Cutler et al. [5]) using step response type dynamic model. State space formulation of MPC was introduced by Li et al. [16].

In the state space framework, the system takes the form:

$$\begin{cases} \dot{x} = f(x, u) \\ x(0) = x_0 \\ t \in [0, +\infty[\end{cases} . \tag{43}$$

Consider the cost function to be minimized

$$J_\infty(u(.), x_0) = \int_0^\infty q(x^u(\tau, x_0), u(\tau))d\tau \tag{44}$$

with

$$x^u(t, x_0) = x_0 + \int_0^t f(x^u(\tau, x_0), u(\tau))d\tau \tag{45}$$

and

$$\begin{cases} q(0,0) = 0, \quad q \in C^2 \\ q(x,u) \geq c_q(||x||^2 + ||u||^2), \quad c_q > 0 \\ u \to q(x,u) \text{ is convex for all } x. \end{cases} \tag{46}$$

Without constraints, Bellman's principle of optimality (1950) gives the solution. In the case of constrained problem, instead of J_∞, we minimize the following cost:

$$J(u(.), x_0, T) = \int_0^T q(x^u(\tau, x_0), u(\tau))d\tau + v(x^u(T, x_0) \tag{47}$$

with

$$J^*(x_0, T) = \underset{u(.)}{min}\ J(u(.), x_0, T) \tag{48}$$

and

$$u^*(t, x_0, T) = \underset{u(.)}{arg\,min}\ J(u(.), x_0, T). \tag{49}$$

This optimization over a finite horizon follows the algorithm:

1. Solve min $J(u(.), x_0, T)$ and find $u^*(., x_0, T)$.
2. Apply $u^*(., x_0, T)$ for $\tau \in [0, T_s[$, $0 \leq T_s \leq T$, (T_s: time sampling period).
3. Repeat using $x(T_s)$ instead of x_0.

6.0.1. *Discrete linear system (basic case).* To explain the method, we consider the discrete linear system:

$$\begin{cases} x(k+1) = Ax(k) + Bu(k) \\ y(k) = Cx(k) \end{cases} \tag{50}$$

where $x(t) \in \mathbb{R}^n$, $u(t) \in \mathbb{R}^m$, $y(t) \in \mathbb{R}^p$ are respectively the state, input and output vectors, and $t = kT_s$. This system (64) results from a discrete system modeling or continuous-discrete transformation. Practical considerations of implementation make this form more appropriate in the framework of MPC.

We suppose that the system is both controllable and observable, and we call $x(k + i/k)$ with $i \geq 0$, the future state vector $x(k + i)$ starting from $t = kT_s$. $x(k+i/k)$ is assumed to be available through using linear state variables estimator. In the case of unconstrained problem, a quadratic cost is minimized in order to obtain optimal control sequence. For instance, choose the following cost:

$$\begin{aligned} J(k) = \sum_{j=k}^{\infty} ((y(j+1/k) - y_{ref})^T Q (y(j+1/k) - y_{ref}) \\ + (u(j/k) - u_{ref})^T R (u(j/k) - u_{ref}) + \Delta u(j/k)^T S \Delta u(j/k)) \end{aligned} \tag{51}$$

with $Q = Q^T \succ 0$, $R = R^T \succeq 0$ and $S = S^T \succeq 0$. The couple (y_{ref}, u_{ref}) corresponds to a set point and $\Delta u(k) = u(k) - u(k-1)$. The solution of this problem is obtained using the LQ controller. In the case of constrained problem,

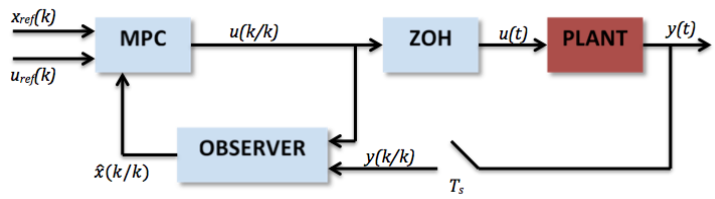

FIGURE 4. General MPC strategy diagram

LQR could not be used to solve control problem. System (50) allows to calculate $x(k+i/k)$, $i = 1, ..., N_r$ at time kT_s, (N_r being the receding horizon length):

$$x(k+i/k) = A^i x(k/k) + \sum_{j=0}^{i-1} A^{i-j-1} B u(k+j/k). \tag{52}$$

The input-output relation along the receding horizon is then:

$$\begin{pmatrix} y(k+1/k) \\ y(k+2/k) \\ \vdots \\ y(k+N_r/k) \end{pmatrix} = \begin{pmatrix} CA \\ CA^2 \\ \vdots \\ CA^{N_r} \end{pmatrix} x(k/k) + \begin{pmatrix} CB & 0 & \cdots & 0 \\ CAB & CB & \ddots & \vdots \\ \vdots & \ddots & \ddots & 0 \\ CA^{N_r-1}B & \cdots & CAB & CB \end{pmatrix} \begin{pmatrix} u(k/k) \\ u(k+1/k) \\ \vdots \\ u(k+N_r-1/k) \end{pmatrix}. \tag{53}$$

Write (53) as

$$\bar{y} = \Psi x(k/k) + \Gamma \bar{u} \tag{54}$$

where $\bar{y}_k \in \mathbb{R}^{pN_r}$, $\bar{u}_k \in \mathbb{R}^{mN_r}$, $\Psi \in \mathbb{R}^{pN_r \times n}$, $\Gamma \in \mathbb{R}^{pN_r \times mN_r}$.

Most frequently used constraints concern the minimum and maximum input, state and output variables:

- The control variables:

$$u_{\min} \leq u(k) \leq u_{\max}. \tag{55}$$

- The change rate of the control variables:

$$\Delta u_{\min} \leq \Delta u(k) \leq \Delta u_{\max} \tag{56}$$

with

$$\Delta u(k) = u(k) - u(k-1). \tag{57}$$

- Soft output variables constraints (relaxed output constraints using large slack variable s_v to avoid constraints conflicts when solving control problem):

$$y_{\min} - s_{v1} \leq y(k) \leq y_{\max} + s_{v1}. \tag{58}$$

- Soft state variables constraints (for the same raison as output constraints):

$$x_{\min} - s_{v2} \leq x(k) \leq x_{\max} + s_{v2} \tag{59}$$

In the case of constrained problem, the cost function (51) becomes:

$$\begin{aligned} J(k) = \sum_{j=k}^{k+N_r-1} & ((y(j+1/k) - y_{ref})^T Q (y(j+1/k) - y_{ref}) \\ & + (u(j/k) - u_{ref})^T R (u(j/k) - u_{ref}) + \Delta u(j/k)^T S \Delta u(j/k)) \end{aligned} \tag{60}$$

subject to (54) and a set of inequality constraints among (55) – (59).

This minimization problem could be expressed as a quadratic cost function subject to linear equality and inequality constraints:

$$\begin{cases} \min\ 1/2\, X^T E X + X^T F \\ \text{subject to} \\ \bar{y} = \Psi x(k/k) + \Gamma \bar{u} \\ MX \leq \gamma \end{cases} \tag{61}$$

and $\bar{y} = C\bar{x}$ with $X = [\bar{x}, \bar{u}]^T$. Clearly, optimization problem (61) is a convex Quadratic Programming (QP) problem; $X^* = [\bar{x}^*, \bar{u}^*]^T$ is than a global minimizer at each iteration. $\bar{u}^*$ being calculated, only $u^*(k/k)$ is applied at time $t = kT_s$ and optimization algorithm is repeated at $t = (k+1)T_s$. In the case of NMPC (Nonlinear Model Predictive Controller), the dynamic is defined using a discretization of the general form (43). Using the same above cost function, optimization problem could be defined as follow:

$$\begin{cases} \min\ \frac{1}{2} X^T E X + X^T F \\ \text{subject to} \\ x(k+i/k) = g(x(k+j/k), u(k+j/k)),\ j = 0, ..., N_r - 1 \\ MX \leq \gamma \end{cases} \tag{62}$$

with $X = [\bar{x}, \bar{u}]^T$. Equality constraint in the optimization problem (62) is nonlinear. Convexity condition in (62) is not guaranteed, then X^* could be a local minimizer. NMPC (Nonlinear Model Predictive controller) is used to solve this problem.
Numerical solution are computed using Active Set, Primal-Dual or SQP methods (Wang [19], Fletcher [10] and Boyd and Vandenberghe [4]).

In the case of force or force-fatigue model, we consider the *more general case* of a varying T_s ($T_s \to I(i)$), then $u(i) = [I(i)\ \eta(i)]^T$, where $I(i) = t(i) - t(i-1)$ is the interpulse between two successive pulses and $\eta(i)$ is the pulse amplitude applied at time t_i. In this case, $\bar{u}(k) = [u(k/k) \ldots u((k+N_r-1)/k)]$ is the discrete receding horizon control vector (of length N_r) to be calculated by the NMPC at time t corresponding to iteration k. Then:

$$\bar{u}(k) = \begin{pmatrix} I(k/k) & I(k+1/k) & \cdots & I((t(N_r))/k) \\ \eta(t_k/k) & \eta((t_k + I(k/k))/k) & \cdots & \eta((t_k + \sum_{j=0}^{N_r-1} I(k+j))/k) \end{pmatrix} \tag{63}$$

$t(N_r)$ being the final time of the optimization horizon which is unknown a priori. For instance, using single move strategy $u(k/k) = u(k+1/k) = \ldots = u((k+N_r-1)/k)$, (see Fig. 5).

The force-fatigue model being nonlinear, an NMPC is used to solve the problem with Nonlinear Programming Algorithm (NPA). In this case, criterion to be minimized is:

$$J(k) = \sum_{j=k}^{k+N_r-1} (F(j+1/k) - F_{ref})^2 \tag{64}$$

subject to: $0 \leq \eta(i) \leq 1$ and $0.01ms \leq I(i) \leq 0.1$.

The estimation of the state variables vector (by the high-gain observer) is used as an initial variables vector to perform the NMPC over the horizon N_r:

ALGORITHM

1. Give $Final_t$, $k = 1$

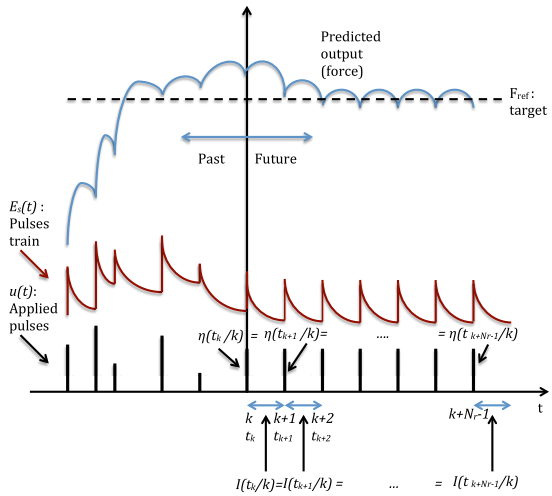

FIGURE 5. *(left half plane)* E_s and force profile for applied amplitude and interpulse stimulation, *(right half plane)* Predicted E_s and force using single move strategy to be optimized.

2. Compute $C_N(t_k)$, $F(t_k)$, $\hat{A}(t_k)$, $\hat{\tau}_1(t_k)$, $K_m(t_k)$
3. $\text{Data}_F = N_r * \frac{u_k(1)}{\text{step}_{int}}$
   with: $u_i(1) = u_k(1)$ for $i = k, k+1, ..., k+(N_r-1)$,
   and step_{int} is a submultiple of $u_i(1) = I_i$.
4. $F_{mean} = \frac{1}{\text{Data}_F} \sum_{j=1}^{\text{Data}_F} F(t_k + j\,\text{Step}_{int}, E_s)$
   with:
$$E_s = \frac{1}{\tau_c} \sum_{i=1}^{k+(N_r-1)} \left(u_i(2) H(t_{N_r} - t_i)\, R_i \exp(-\frac{t_{N_r} - t_i}{\tau_c}) \right). \tag{65}$$
   We recall $u_i(1) = u_k(1)$ and $u_i(2) = u_k(2)$ for $i = k, k+1, ..., k+(N_r-1)$, (single move profile) and $t_i = t_{i-1} + u_{i-1}(1)$, $i \geq 2$, $t_{N_r} = \sum_{i=1}^{k+(N_r-1)} I_i$.
5. $u^*(k/k) = \begin{pmatrix} I_k^* \\ \eta_k^* \end{pmatrix} = \underset{\substack{I_k \in [I_{min}, I_{max}] \\ \eta_k \in [\eta_{min}, \eta_{max}]}}{arg\,min} \quad J$
6. if $t_{k+1} \geq \text{Final}_t \Rightarrow$ stop, else, $k = k+1$, back to 2.

7. Numerical results.

7.1. **High-gain observer.** To exhibit the interest of the use of the power m in the nonlinear observer, let's consider MPC based nonlinear observer using only amplitude as control variable. We consider also the worst case of +30% of error of K_m.

The following simulation results follow the stimulation protocol used in practise (a set of periods with stimulation and rest time slots in each period). During the stimulation time slot, the control is calculated to bring the force to F_{ref} and in the rest time slot, the stimulation amplitude is set to 0. In this section, only two stimulation periods are considered.

In the cases of interpulse $I = 10ms$ $(100Hz)$ and $I = 25ms$ $(40Hz)$, the power values are $m = 3$ and $m = 5$, respectively. Fig.6 and Fig.7 represent the A estimates for $I = 10ms$ and $I = 25ms$, respectively. Fig.8 and Fig.9 are the τ_1 estimates for $I = 10ms$ and $I = 25ms$. $\hat{A}$ converges after $50ms$ when $I = 10ms$ and $100ms$ when $I = 25ms$. Concerning $\hat{\tau}_1$, it converges after $75ms$ when $I = 10ms$ and $200ms$ when $I = 25ms$. Large I seems to delay the convergence of the observer.

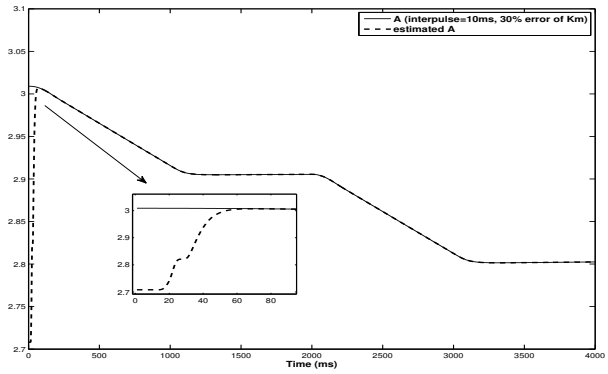

FIGURE 6. Evolution of A and $\hat{A}$ for $I = 10$, 30% error of K_m.

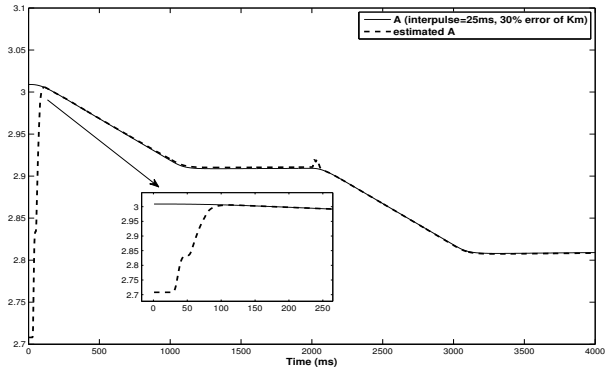

FIGURE 7. Evolution of A and $\hat{A}$ for $I = 25$, 30% error of K_m.

Fig.10 represents the force response for amplitude control strategy (for a receding horizon $N_r = 10$) based on the proposed observer for $I = 25ms$ and a force reference of $250N$. Force mean value converges to the force reference after $200ms$.

7.2. **MPC with interpulse and amplitude as control variables.** In this section, five stimualtion periods are presented (due to the experiment protocol). Figures 11, 14 and 15 are the force response in the case of $F_{ref} = 425N$ and $(N_r = 3, 5, 10)$, the interpulse and the amplitude controls for $N_r = 10$, respectively. As expected, $N_r = 10$ gives the best regulation performances (response time and overshoot).

Before $t = 6000ms$ with $N_r = 10$, the force is correctly maintained at $F_{ref} = 425N$. For $t \geq 6000ms$ (starting from the forth period), the fatigue level A is very high so

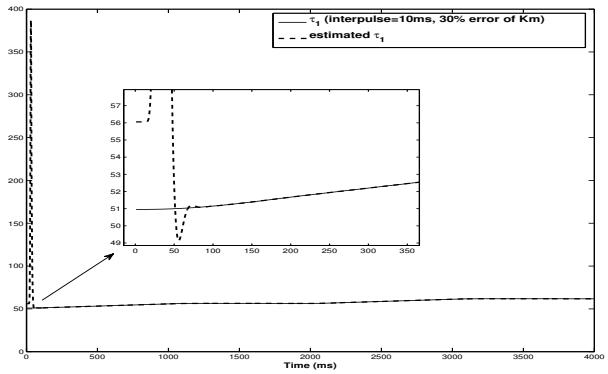

FIGURE 8. Evolution of τ_1 and $\hat{\tau}_1$ for $I = 10$, 30% error of K_m.

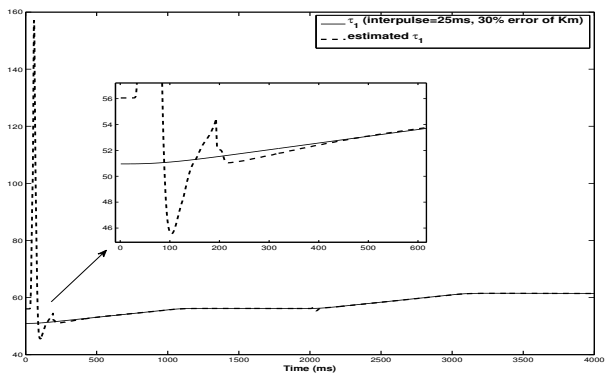

FIGURE 9. Evolution of τ_1 and $\hat{\tau}_1$ for $I = 25$, 30% error of K_m.

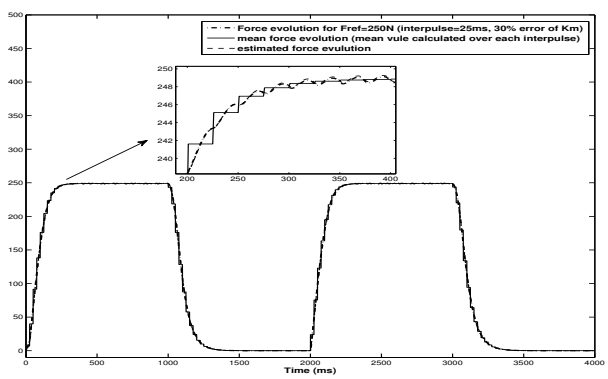

FIGURE 10. Evolution of F, $\hat{F}$ and F mean value over I for $I = 25$, 30% error of K_m, $Fref = 250N$.

that maximum value of amplitude control (see Fig. 15) and computed interpulse control (see Fig. 14) cannot maintain F at F_{ref}. Maximum interpulse frequency is not used at the beginning of the forth and the fifth periods. Higher value of N_r

could correct this problem (supposing that global minimizer of MPC algorithm is reached at each iteration). However, increasing N_r will render MPC algorithm time consuming which causes a problem for real time implementation.

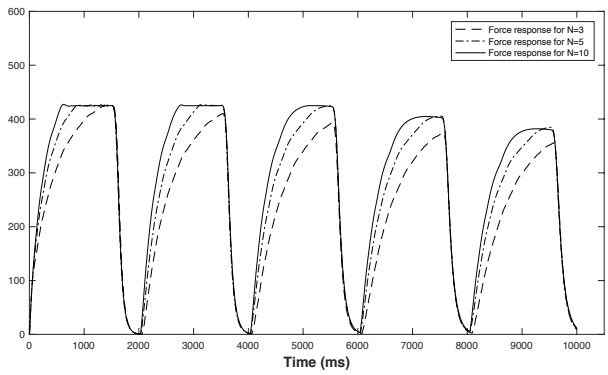

FIGURE 11. Evolution of the force for a reference force of $425N$ and different receding horizons $(3, 5$ and $10)$

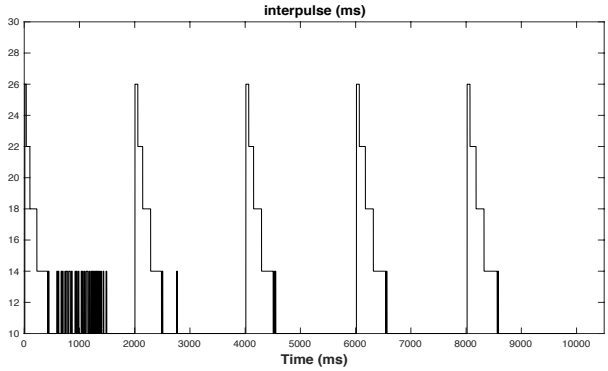

FIGURE 12. Evolution of the interpulse (control) for a reference force of $425N$ and a preditive horizon of 10.

8. **Conclusion.** This work deals with the estimation of the state variables of the Ding et al. force-fatigue model where the control is the interpulse and/or amplitude of the electrical stimulation. Preliminary geometric analysis of the force control controlling force level is presented with the aim of a future PMP control strategy. In the case of a fixed interpulse, the proposed high-gain observer using the force measurements exhibits the relation between the interpulse and the parameter m to perform accurate variables estimation. Model Predictive Control (MPC) strategy is presented in the case of both stimulation interpulse and amplitude as control variables. To test MPC-(high-gain observer) efficiency, simulation results of the force evolution controlled by stimulation amplitude are presented. This control is based on the state variables estimation to perform accurate prediction over the receding horizon and then to bring the force to a reference force value. The final set

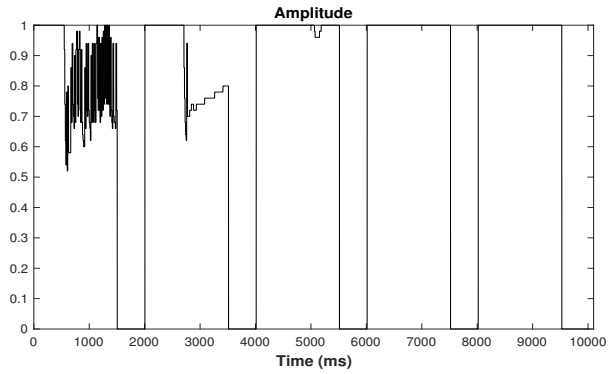

FIGURE 13. Evolution of the amplitude (control) for a reference force of $425N$ and a preditive horizon of 10.

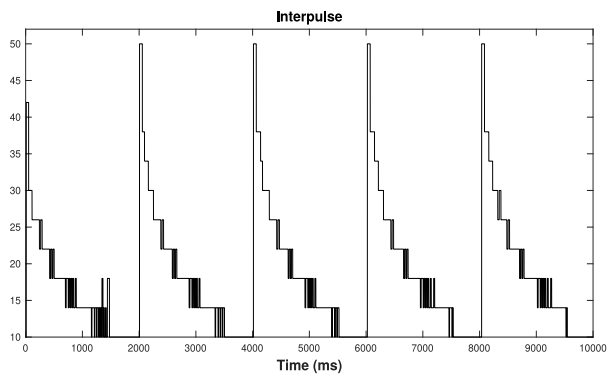

FIGURE 14. Evolution of the interpulse (control) for a reference force of $425N$ and a preditive horizon of 10.

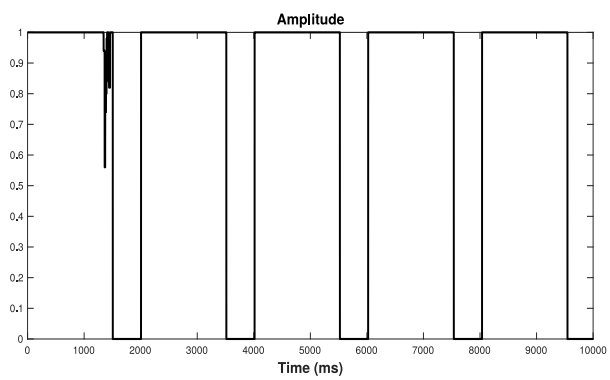

FIGURE 15. Evolution of the amplitude (control) for a reference force of $425N$ and a preditive horizon of 3.

of stimulations is dedicated to the control of the force level using both stimulation interpulse and amplitude controls. These simulations show the effect of the receding horizon on the control efficiency. Reasonable value of N_r is however suitable to guarantee a short computation time for real time implementation.

REFERENCES

[1] T. Bakir, B. Bonnard and S. Othman, *Predictive control based on nonlinear observer for muscu lar force and fatigue model*, ACC 2018 - American Control Conference, Milwaukee (2018), preprint hal-01591187

[2] J. Bobet and R.B. Stein *A simple model of force generation by skeletal muscle during dynamic isometric contractions*, IEEE Transactions on Biomedical Engineering, **45** (1998) 1010–1016

[3] L. Bourdin and E. Trélat, *Optimal sampled-data control, and generalizations on time scales*, Math. Cont. Related Fields, **6** (2016) 53–94

[4] S. Boyd and L. Vandenberghe, *Convex Optimization*, Cambridge University Press (2004)

[5] C.R. Cutler and B.L. Ramaker, *Dynamic matrix control: A computer control algorithm*, In Joint automatic control conference, San Francisco, **17** (1981)

[6] J. Ding, S.A. Binder-Macleod and A.S. Wexler, *Two-step, predictive, isometric force model tested on data from human and rat muscles*, J. Appl. Physiol., **85** (1998) 2176–2189

[7] J. Ding, A.S. Wexler and S.A. Binder-Macleod, *Development of a mathematical model that predicts optimal muscle activation patterns by using brief trains*, J. Appl. Physiol., **88** (2000) 917–925

[8] J. Ding, A.S. Wexler and S.A. Binder-Macleod, *A predictive model of fatigue in human skeletal muscles*, J. Appl. Physiol., **89** (2000) 1322–1332

[9] J. Ding, A.S. Wexler and S.A. Binder-Macleod, *Mathematical models for fatigue minimization during functional electrical stimulation*, J. Electromyogr. Kinesiol., **13** (2003) 575–588

[10] R. Fletcher, *Practical Methods of Optimization, Volume 2, Constrained Optimization*, Springer, New York (1981)

[11] J.P. Gauthier, H. Hammouri and S. Othman, *A simple observer for non linear systems Application to bioreactors*, IEEE Trans. Automat. Control, **37** (1992) 875–880

[12] R. Gesztelyi, J. Zsuga, A. Kemeny-Beke, B. Varga, B. Juhasz and A. Tosaki, *The Hill equation and the origin of quantitative pharmacology*, Arch. Hist. Exact Sci., **66**(4) (2012), 427–438

[13] R. Hermann, J. Krener, *Nonlinear controllability and observability*, IEEE Transactions on Automatic Control, AC–**22** (1977) 728–740

[14] A. Isidori, *Nonlinear Control Systems*, 3rd ed. Berlin, Germany: Springer-Verlag (1995) xvi+549

[15] L.F. Law and R. Shields, *Mathematical models of human paralyzed muscle after long-term training*, Journal of biomechanics, **40** (2007) 2587–2595

[16] S. Li, K.Y. Lim and D.G. Fisher, *A state space formulation for model predictive control*, Springer, New York, **35**, no.2 (1989) 241–249

[17] J. Richalet, A. Rault, J. Testud and J. Papon, *Algorithmic control of industrial processes*, In 4th IFAC symposium on identification and system parameter estimation (1976) 1119–116

[18] H.J. Sussmann and V. Jurdjevic, *Controllability of nonlinear systems*, J. Differential Equations, **12** (1972) 95–116

[19] L. Wang, *Model Predictive Control System Design and Implementation Using MATLAB*, Springer, London (2009)

[20] E. Wilson, *Force response of locust skeletal muscle*, Southampton University, Ph.D. thesis (2011)

[21] M. Yochum, *Contribution à la conception d'un électromyostimulateur intelligent*, Thèse de doctorat, Instrumentation et informatique de l'image Dijon (2013).

Received xxxx 20xx; revised xxxx 20xx.

E-mail address: bernard.bonnard@u-bourgogne.fr
E-mail address: toufik.bakir@u-bourgogne.fr
E-mail address: jeremy.rouot@epf.fr